

# INTERACTION BETWEEN SHEAR AND NORMAL STRESS AT CONCRETE-FRP INTERFACE

Filippo Bastianini<sup>1</sup>, Barbara Bonfiglioli<sup>2</sup>, Claire Verlinden<sup>3</sup> and Giovanni Pascale<sup>2</sup>

<sup>1</sup> DCA, IUAV, University of Venezia, S.Croce 191, Tolentini - Venezia, Italy.

<sup>2</sup> DISTART, Department of Structural Engineering, University of Bologna, Viale Risorgimento, 2, I 40136 Bologna, Italy.

<sup>3</sup> GTGC, Department of Geotechnical and Civil Engineering, Polytech Lille, Villeneuve d'Ascq, France

## ABSTRACT

Debonding between external FRP strengthening and concrete substrate is an important limiting factor for the complete exploitation of the achievable strength upgrade, being itself the main cause of premature brittle failure of the strengthened member both in flexural and shear modes. Small unlevelled parts of the strengthened surface and substrate cracks characterized by slipping borders are typical discontinuities usually present in real applications and they may act as nucleation centres for debonding phenomena by creating a combination of shear and normal stress that strongly affects the bonding failure. Since different failure mechanisms become possible varying the ratio between shear and normal stress, around these discontinuities the failure may be driven out from the resin shear failure domain and into the concrete tension failure domain, causing a dramatic change in the typical strength that facilitates debonding initiation. Other parameters, such as the surface roughness of the concrete substrate, contribute to influence the phenomenon. This experimental research is aimed to investigate the bonding strength dependence on the ratio between normal stress and shear stress, and it was carried out through a pull-off test set up modified in order to obtain loading at various inclinations between 15° and 90° with respect to the strengthening surface. The test programme includes various types of concrete surface and two different types of resin as well. A series of preliminary tests allowed the first author to obtain failure envelopes that well distinguish different failure mechanisms regarding both the concrete and the resin. In this research a greater number of tests have been performed and some additional parameters have been taken into account in order to allow a sensitivity analysis of the affecting factors.

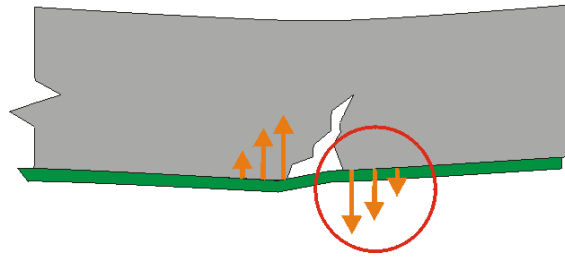
## 1. INTRODUCTION

External Bonded Reinforcement (EBR) are finding ever-increasing use in structural engineering even if their efficiency is strongly affected by the mechanisms at the FRP-concrete interface. The complexity of these mechanisms influences the local phenomena which have to be understood and correctly predicted in order to obtain a reliable evaluation of safety margins of the rehabilitation design with respect to both ultimate and serviceability limit states. In literature, some studies can be found concerning these local phenomena. So research is still in progress and takes into account both linear and non-linear features of the problem. The experimental investigations of the efficiency and quality of the EBR applications are still in progress [Bastianini et al., 2002; Bastianini, 2001; Pascale et al., 2000].

Coexistence of normal and shear stress at the FRP-concrete interface is recognized as one of the main causes capable of catalysing local debonding of external composite strengthenings. Being this sort of anomalies frequently associated to premature brittle failure of most FRP strengthened members, a deeper comprehension of its mechanics seems to be of a certain interest.

From various experimental investigations, see i.e. [Aiello and al., 2001] in which FRP strengthened concrete arches with different curvatures exhibited premature peeling failure when the ratio between normal and shear stress overcame certain values, it has been noted that debonding is preferentially initiated around some sort of surface discontinuities such as small unlevelled areas and substrate cracks in which some slipping of the borders out of the strengthening plane occurred (Fig.1).

Intuitive explanation of this catalyst effect is proposed taking into account the geometric effect that is responsible of a normal stress distribution in the neighbourhood of the discontinuity. The combination of the tensile normal stress with the transfer shear stress at the interface is here addressed as the responsible of the failure initiation.



“Fig. 1. local normal stresses around a substrate crack with border slipping out of the strengthening plane.”

## 2. EXPERIMENTAL PROGRAMME

The experimental programme has been performed at LaRM (Materials Testing Laboratory) – Department DISTART of University of Bologna.

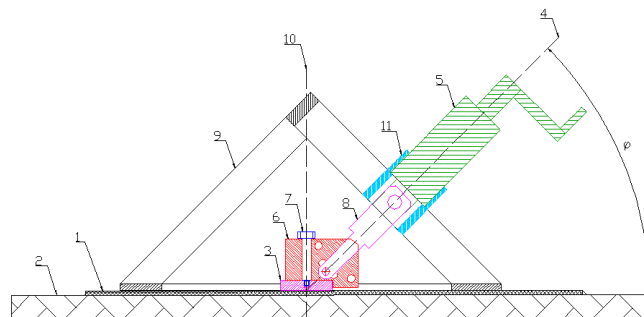
### 2.1 Test fixture

A special test fixture, schematically shown in the section view of Fig. 2, was designed in order to accommodate a C-104 CAPO test hydraulic pull-machine manufactured by Germann Instruments S.A. (Emdrupvej 102, Copenhagen, Denmark). Referring to the section view, the steel frame (9), secured to the concrete slab with up to four 8 mm screw anchors (not shown), provides counterpressure resting to the pull-machine (5), which can be accommodated into the sleeve (11) that is fastened to the frame at a proper tilt angle  $\varphi$  with respect to the strengthening plane. The connecting rod (8) is hinged to the mobile head of the pull-machine at one end, and to one of the proper holes fitting plate (6) at the other end, with respect with the tilt angle  $\varphi$  chosen for the sleeve position.

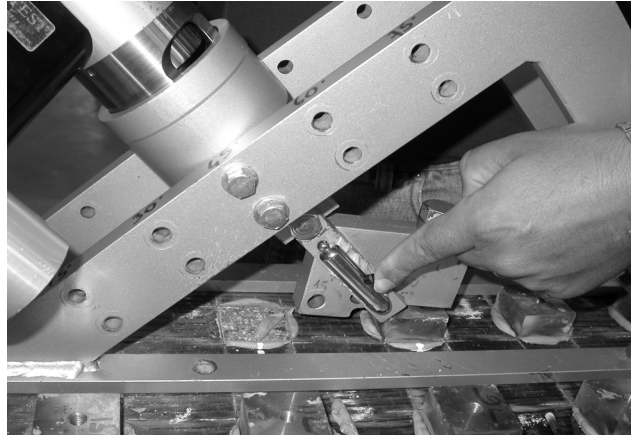
Fitting plate (6) is connected to the test plate (3) trough a cylindrical hinge realized by the special screw fastener (7), leaving free the plate rotation around the vertical axis (9).

The test plate (3) is glued to the surface of the FRP strengthening layer (1) which is itself bonded onto the concrete substrate (2). Elements (6), (7) and (8) are properly dimensioned in order to ensure the following conditions:

- load is applied along a barycentric direction with respect to the test plate (3) bottom surface;
- load direction has a tilt angle  $\varphi$ ;
- no bending load or torque around vertical axis (10) are present.



“Fig. 2. schematic section view of the tilt pull-off test fixture.”



“Fig. 3. laser pointer system used to check tilt angle trimming”

Fine trimming of the tilt angle has been provided through a tuning screw (not shown) controlling the clearance between the fitting plate (6) and the test plate (3), and barycentricity has been checked using a laser pointer coaxially installed on the connecting rod (8) (Fig. 3).

## 2.2 Test specimens

The programme was based both on tilt and normal pull-off tests. They have been performed on some concrete slabs of 100 cm length and 25 cm width, strengthened with Carbon Fiber Reinforced Polymer (CFRP). Steel rigid plates with 40x40 mm surface and 20 mm thickness were bonded on the FRP with epoxy adhesive after surface cleaning with abrasive and alcohol degreasing. Tests with 7 different angles (15°, 30°, 45°, 60°, 75°, 90°) have been carried out. Ten tests have been performed for each angle. The mechanical properties of all the materials (concrete, resin and FRP) have been experimentally determined and are reported in Table 1. FRP has been cutted around the plate border before testing, contextually ensuring the etching of the concrete substrate for a depth of 1 mm. Some more tests have been carried out on different specimens, with different types of concrete surface roughness, as well as different types of epoxy resin. A doughy resin have been used too.

“Table 1: Mechanical properties of materials.”

| Property             | Value        |
|----------------------|--------------|
| Concrete             |              |
| Young's modulus      | 268800 [MPa] |
| Poisson ratio        | 0.25 [--]    |
| Compression strength | 40.5 [MPa]   |
| Tensile strength     | 4.5 [MPa]    |
| Resin                |              |
| Young's modulus      | 2626 [MPa]   |
| Poisson ratio        | 0.35 [--]    |
| Tensile strength     | 37 [MPa]     |
| CFRP                 |              |
| Young's modulus      | 239090 [MPa] |
| Poisson ratio        | 0.35 [--]    |
| Tensile strength     | 2674 [MPa]   |

### 3. EXPERIMENTAL RESULTS

Data collected through tilt pull-off and normal pull off, in terms of mean normal strength vs. mean shear strength, can be plotted to obtain a curve conceptually similar to a failure domain (pseudo-failure domain).

#### 3.1 Evaluation of the normal and shear stress

Actual failure load ( $F = F(\varphi)$ ) is calculated according to eq. [1] as the fraction of the peak force applied from the pull-machine ( $P$ ) that is transmitted along the connecting rod and applied at the barycenter of the bottom surface of the test plate. The remaining part ( $R$ ) is instead discharged onto the substrate through the counterpressure frame. By simple algebra considerations, we obtain

$$F = \frac{P}{\cos\left|\frac{\pi}{4} - \varphi\right|} \quad (1)$$

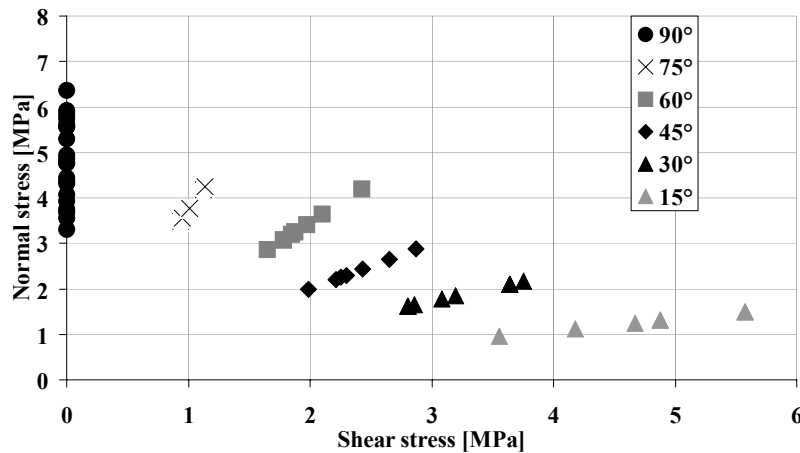
Then, average normal stress  $\sigma_{mean}$  and average shear stress  $\tau_{mean}$  at failure are calculated according to [2] and [3], respectively, being  $a$  the test plate section side.

$$\sigma_{mean} = \frac{F}{a^2} \sin \varphi \quad (2)$$

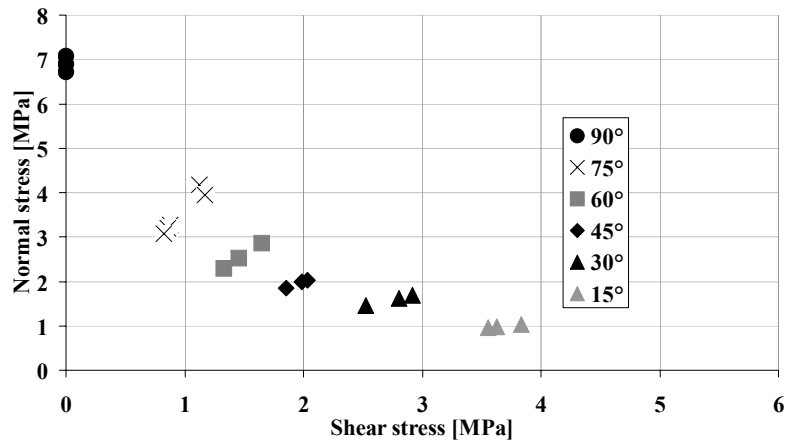
$$\tau_{mean} = \frac{F}{a^2} \cos \varphi \quad (3)$$

#### 3.2 Experimental diagrams and comments

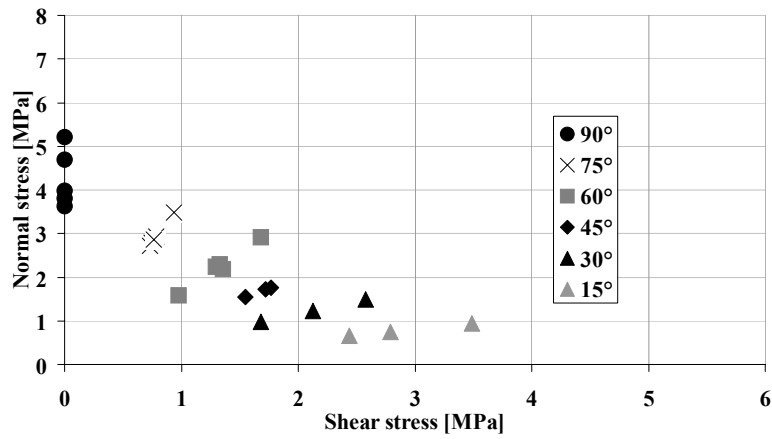
In Fig. 4, Fig. 5 and Fig. 6, the diagrams of shear stress vs. normal stress are plotted for the concrete slabs with fluid resin and smooth surface, with fluid resin and rough surface and with doughy resin and smooth surface, respectively.



“Fig. 4. Shear stress vs. Normal stress for concrete slab with fluid resin and smooth surface.”



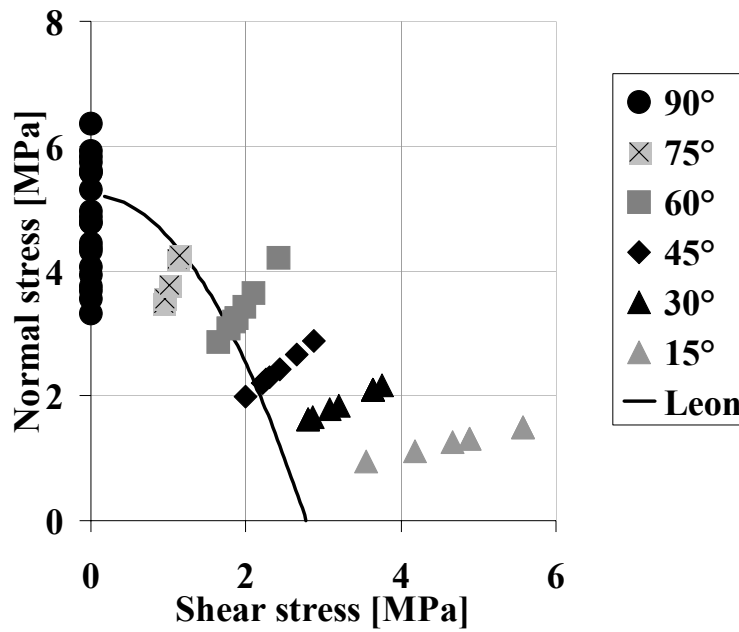
“Fig. 5. Shear stress vs. Normal stress for concrete slab with fluid resin and rough surface.”



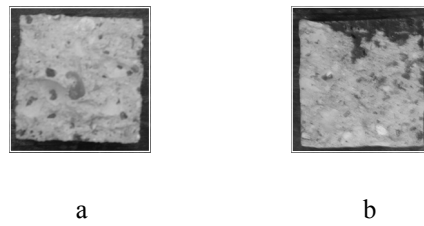
“Fig. 6. Shear stress vs. Normal stress for concrete slab with doughy resin and smooth surface.”

From the simple comparison between the experimental data obtained with both smooth and rough surface, it appears clear that the shear strength decreases strongly when the normal tensile stress increases.

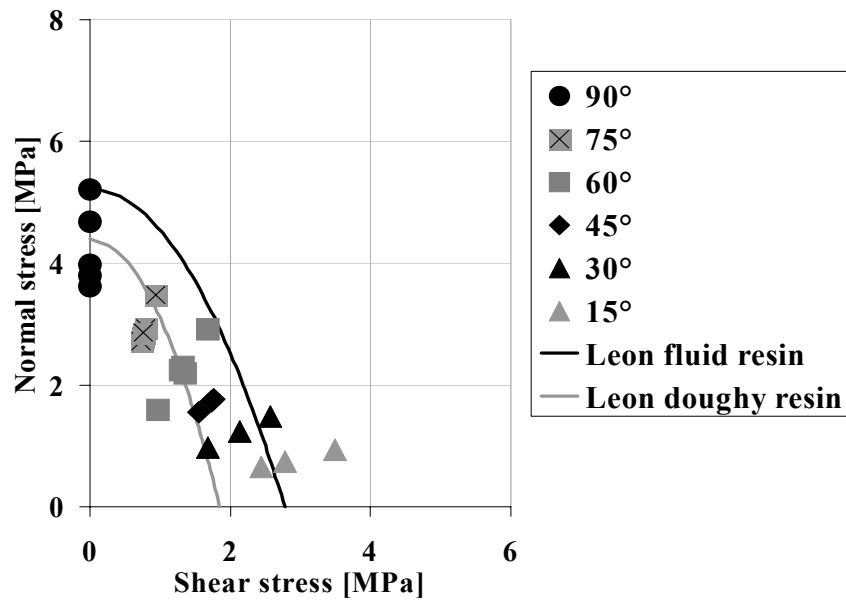
About the influence of the kind of resin used, the choice of doughy resin induces both normal and shear strength decreasing. This confirms that the interface behaviour is affected by both concrete and resin properties.



“Fig. 7. Leon bonding failure domain obtained from the experimental results (angle’s value between 45° and 90°) for the fluid resin”



“Fig. 8. Experimental failure modes.”



“Fig. 9. Leon bonding failure domain obtained from the experimental results (angle’s value between 45° and 90°) for the doughy resin, compared with the Leon failure domain obtained for fluid resin.”

In Fig. 4, a pronounced growth of the pulling force can be noted for the lower angles (15° and 30°). In effect the failure modes observed experimentally outlined that for the higher values the crisis is located mainly in the concrete (see Fig. 8a); while, for lower angles it interests the resin-concrete interface (see Fig. 8b). For this reason, in Fig. 7, the bonding failure pseudo-domain is plotted for the slab with fluid resin and smooth surface, taking into account only the experimental results obtained for tilt angles between 45° and 90°. In this way it appears clearly that for lower angles the failure mechanism is considerably influenced by the resin properties.

The failure pseudo-domain has been calculated according to the Extended Leon model [Etse & William, 1994], using the formula (4), where the parameters have been determined as  $a = -1.480$  and  $b = 7.725$ :

$$\tau_u = (a\sigma_u + b)^{1/2} \quad (4)$$

In Fig. 9, the analogous failure pseudo-domain is represented for the slab with doughy resin and smooth surface, starting from the experimental data. It has been calculated according to the Extended Leon model ( $a = -0.779$ ;  $b = 3.416$ ). The failure pseudo-domain obtained for the slab with fluid resin and smooth surface is plotted too. Considering only the Leon curve calculated for the doughy resin, the same phenomenon is observed: for higher values of the pulling angles the experimental points move far from the failure pseudo-domain, according to the previous results.

By comparing the two Leon failure pseudo-domains, it can be noted that the behaviour at the concrete-FRP interface is not only dependently by concrete properties, because in the last case the two failure pseudo-domains have to be coincident.

#### 4. CONCLUSION

This paper addresses an experimental investigation of FRP-concrete interface behaviour. It deals with great number of both pull-off and tilt pull-off tests on concrete slabs strengthened with CFRP with different resins and surfaces.

A adequate experimental set-up to define a pseudo failure domain for FRP-concrete interface has been designed and validated.

From the experimental results it was possible to detect a failure pseudo-domain of FRP-concrete interface, well described by the Leon law. The changes of the pseudo-domain seem suitable to detect the differences due to the variation of the resin's properties. So further investigations will be able to adequately correlate the Leon's parameters with the features of both resin and concrete.

If the failure domain of the resin, approximated by the envelope of Mohr's circles, is taken into account, a really high distance can be noted between the bonding failure domains of concrete and resin, so it can be concluded that the most important role at FRP-concrete interface is played by concrete properties.

#### ACKNOWLEDGEMENT

Our thanks to all the staff of the Material Testing Laboratory of the University of Bologna, for their diligence in realising the experimental programme. The financial support of the European Erasmus/Socrates programme, of Autobrennero S.p.A and of MIUR, Italian Ministry of University and Research (Contract n° 2002085488-009) are also gratefully acknowledged.

This research topic is related to the activity of the Centre "Michele Capurso" of Study and Research for Identification of Materials and Structures (CIMEST).

## References

1. **Bastianini F., Di Tommaso A., Pascale G.** “Ultrasonic Non-Destructive Assessment of Bonding Defects in Composite Structural Strengthenings”, Proc. Of 4th PhD Civil Eng. Symp., Munchen, (2002).
2. **Bastianini F.** “Non-destructive techniques for quality assessment and monitoring of composite strengthenings”, Composite Structures, Vol. 53 No. 4, pp. 463-467 (2001).
3. **Pascale G., Bonfiglioli B., Bastianini F.**, “Metodologie di indagine per la valutazione della qualità dei rinforzi in FRP applicati a strutture in calcestruzzo e altri materiali”, Atti del XXIX Convegno Nazionale dell’Associazione Italiana per l’Analisi delle Sollecitazioni, Lucca, 6-9 settembre 2000, pp. 739-748.
4. **Aiello M.A., Galati N., La Tegola A.**, “Bond analysis of curve structural concrete elements strengthened using FRP materials”, Proc. of FRPRCS5 International conference, July 16-18, Cambridge UK, (2001).
5. **Etse G. and Williams K.**, “A fracture energy formulation for inelastic behavior of plain concrete”, ASCE J. of Eng. Mech., 120, 9, pp. 1983-2011, (1994).